

Supplementary information

Carbon and sediment fluxes inhibited in the submarine Congo Canyon by landslide-damming

In the format provided by the authors and unedited

1 **Extended Data Figures**

2 Extended Data Figure 1. Two other possible canyon-flank landslides identified in the 2019 bathymetry.

3 a) Possible landslide headscarp and deposit which are interpreted to have involved similar processes

4 to those envisaged for the canyon-flank landslide seen in Fig. 2. b) Canyon-flank landslide appears to

5 constrict the canyon floor leading to the development of a new thalweg channel due to enhanced

6 turbidity current erosional capacity. Processes envisaged here are similar to those described in Fig. 4a,

7 c.

8

9

10 **Supplementary material**

11 **SM1. Other possible canyon-flank landslides in the 2019 data**

12 Other features visible in the 2019 bathymetry data are also interpreted as potential canyon-flank
13 landside deposits (SFig. 1). However, in neither case did the canyon-flank landslide occur between
14 2005 and 2019. Therefore, we cannot say for certain that the interpreted morphology is a
15 consequence of a canyon-flank landslide. A first possible headscarp and deposit, with similar
16 morphologies to that seen in the upper part of the study area (Fig. 2b), are located at 1980 m water
17 depth on the northern canyon-flank (SFig. 1a). If indeed a canyon-flank landslide, the headwall is 200
18 m high and 290 m wide with a perimeter of 1.73 km. Here, the main canyon thalweg is situated
19 between the landslide headscarp and the interpreted deposit. The shape of the infill is suggestive of
20 a palaeo-meander which has been cut-off.

21 A second potential landslide complex with a different morphology is observed at 1300 m water depth
22 on the northern canyon-flank, at the eastern end of the study area (SFig. 1b). Here, multiple
23 headscarps are associated with a lobate deposit covering 0.65 km². The deposit constricts the canyon
24 thalweg, but does not block it. A channel, which has been incised into the canyon floor meanders
25 around the landslide deposit with a knickpoint up-canyon of the deposit (SFig. 1b). The channel is 6
26 km long with a maximum depth and width of 10 and 200 m, respectively. We interpret the processes
27 associated with this canyon-flank landslide to be similar to those described in Fig. 4a, c.

28

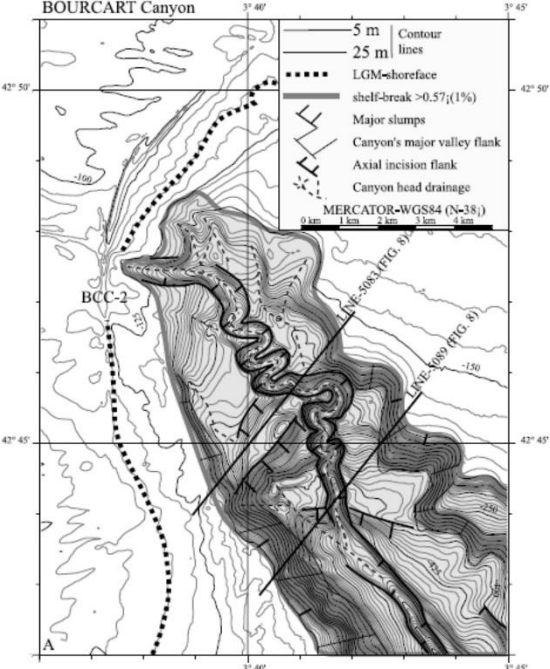
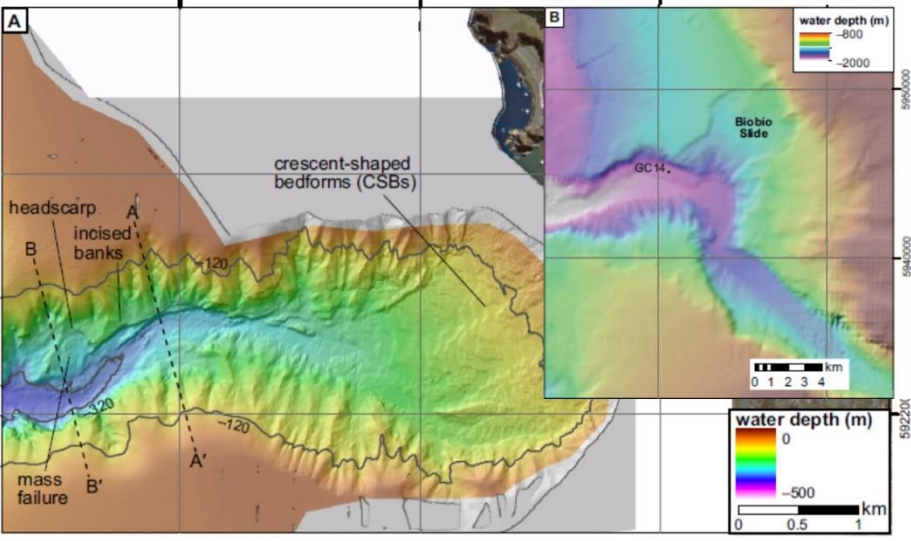
29 **Supplementary Tables**

30 Supplementary Table 1. Submarine canyons where high resolution multibeam bathymetry is available.
31 Studies which include repeat multibeam bathymetry similar to this study are identified. Mass wasting
32 features, terraces and canyon sidewalls similar to those observed in this study are described.
33 Bathymetry examples of the described features are also shown. For example, terraces are identified
34 which are likely to be areas of high sediment accumulation, and may be prone to collapse. Other
35 examples where submarine canyons exhibit similar seafloor geomorphic features in 3-D seismic data,
36 such as the Niger Channel, but where bathymetric data has not been published have been omitted.

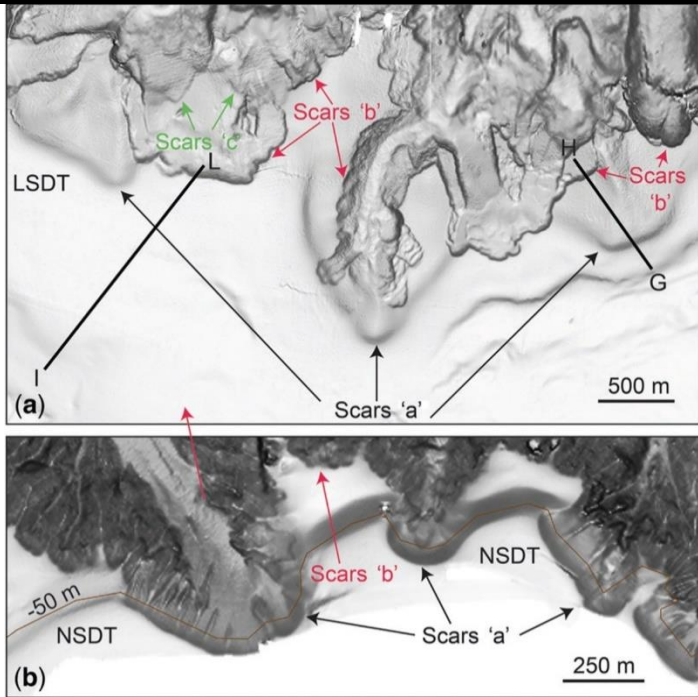
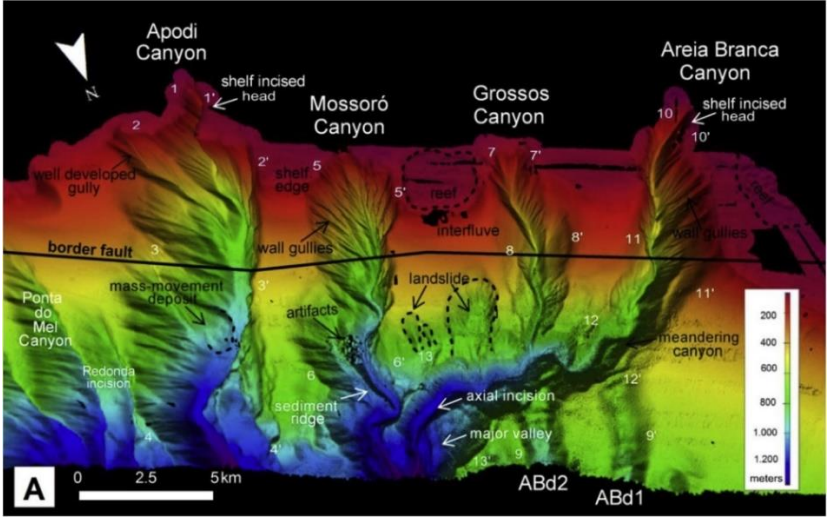
37

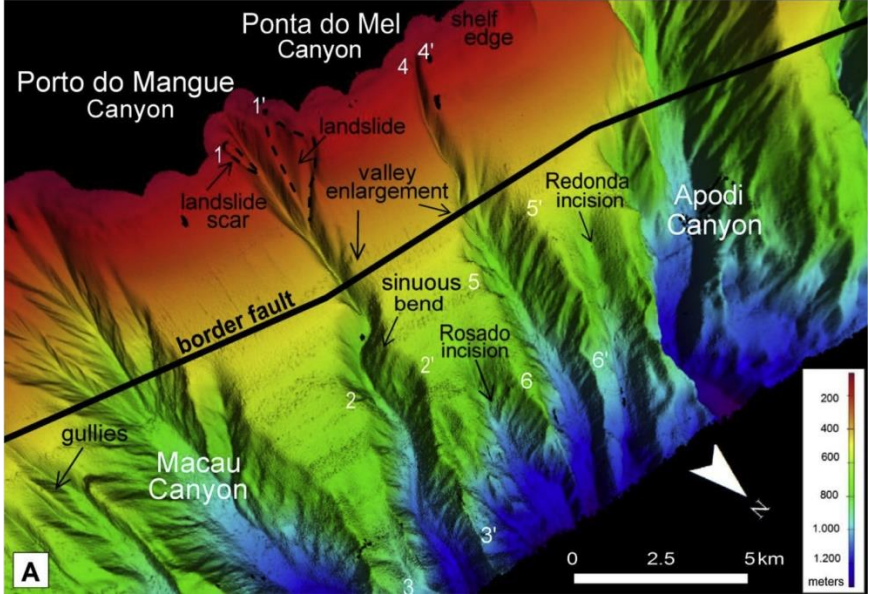
Canyon/ Margin	Date of Survey	Multibeam bathymetry resolution (m)	Reference	Description of mass wasting or terrace features	Swath bathymetry of submarine canyon showing similar landslide or terrace features as identified in the Congo Canyon
Dohrn	2000 - 2014	10	Aiello et al. 2020 ⁵¹	Landslide scars located around the rim of the canyon. Additional slope failure deposits identifiable in seismic profile data	
Magnaghi	2000 - 2014	10	Aiello et al. 2020 ⁵¹	Slope failure deposits identifiable in seismic profile data	

Andøya	2004, 2005	5 (shallower than 1000 m) 25 (deeper than 1000 m)	Amundsen et al. 2015 ⁵² Laberg et al. 2007 ⁵³	Landslide headwalls visible in bathymetry.	
Cap Timiris	2003	Not reported	Antrobreh and Krastel 2006 ⁵⁴	Slump deposits identifiable in canyon thalweg from steep canyon walls. Similar arcuate terrace features to Congo Canyon	

Bourcart	1995 – 2002	Not reported	Baztan et al. 2005 ⁵⁵	Slide headwalls visible in bathymetry and seismic cross sections	 <p>The figure is a bathymetric map of Bourcart Canyon. It features contour lines at 5 m and 25 m intervals. A dashed line represents the LGM-shoreface, and a thick black line indicates a shelf-break with a slope greater than 0.57 (1%). The map identifies major slumps, the canyon's major valley flank, axial incision flanks, and the canyon head drainage. A specific location is marked as BCC-2. The map uses a Mercator-WGS84 projection (N=38) and includes a scale bar from 0 to 4 km. Geographic coordinates range from 3° 40' to 3° 45' longitude and 42° 45' to 42° 50' latitude.</p>
Biobío	2011	5	Bernhardt et al. 2015 ⁵⁶	<p>Arcuate headscarps present with hummocky material partially blocking the canyon.</p> <p>Additional detachment surfaces are visible in</p>	 <p>The figure shows a bathymetric map of Biobío Canyon. It highlights features such as headscarps, incised banks, mass failure zones, and crescent-shaped bedforms (CSBs). A specific location is marked as gc14. The map includes a scale bar from 0 to 4 km and a color-coded water depth scale from 0 to -2000 meters. Geographic coordinates are provided along the axes, ranging from 660000 to 664000 longitude and 5922000 to 5960000 latitude.</p>

				seismic profiles																	
Cap Lopez	2004 – 2008 (repeat bathymetry)	10	Biscara et al. 2013 ⁵⁷	Canyon flank landslide identified. Estimated mass of $95,000 \text{ m}^3 \pm 15,000 \text{ m}^3$. 60% of thalweg deposit reworked within one year.	<p>A 2006-2007</p> <p>Landslide headscarp</p> <p>Landslide deposit</p> <p>Sediment thickness (m)</p> <table border="1"> <tr> <th>Erosion</th> <th>Deposition</th> </tr> <tr> <td>> 20</td> <td>1-2</td> </tr> <tr> <td>15-20</td> <td>2-4</td> </tr> <tr> <td>10-15</td> <td>4-6</td> </tr> <tr> <td>5-10</td> <td>> 6</td> </tr> <tr> <td>4-5</td> <td></td> </tr> <tr> <td>2-4</td> <td></td> </tr> <tr> <td>1-2</td> <td></td> </tr> </table> <p>Bathymetry (m)</p> <p>0 to 100</p> <p>B 2006-2008</p>	Erosion	Deposition	> 20	1-2	15-20	2-4	10-15	4-6	5-10	> 6	4-5		2-4		1-2	
Erosion	Deposition																				
> 20	1-2																				
15-20	2-4																				
10-15	4-6																				
5-10	> 6																				
4-5																					
2-4																					
1-2																					

Cape D'Orlando Basin	2011, 2012	1 (0 – 100 m water depth) 20 (100 – 1000 m water depth)	Casalbore et al. 2020 ⁵⁸	280 landslide scars recognised in bathymetry down to 550 m water depth.	
Areia Branca	2011	50	de Almedia et al. 2015 ⁵⁹	Arcuate headwalls with the presence of marginal terraces	
Grossos	2011	50	de Almedia et al. 2015 ⁵⁹		
Mossoro	2011	50	de Almedia et al. 2015 ⁵⁹	Landslide scars on canyon walls.	

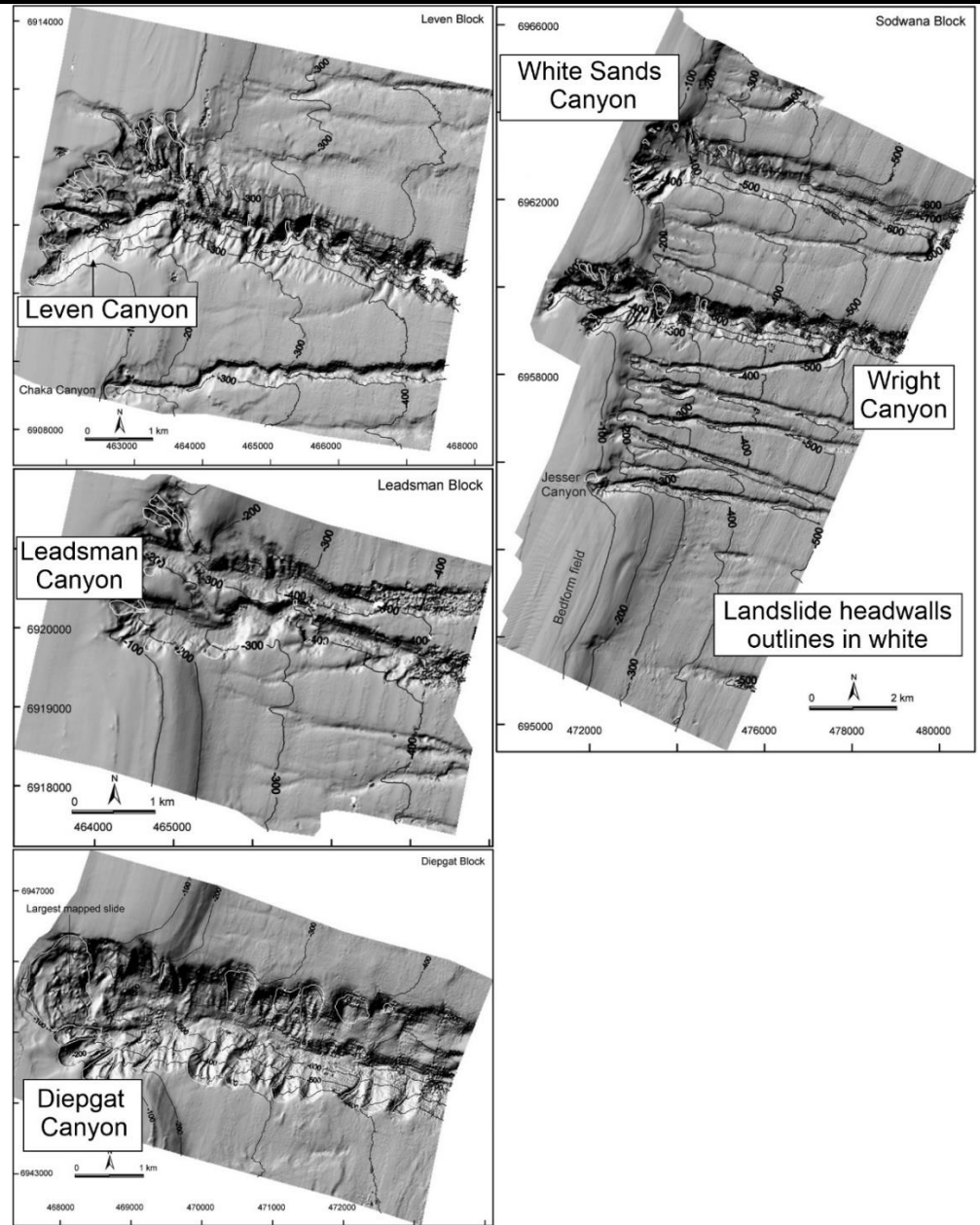
Apodi	2011	50	de Almedia et al. 2015 ⁵⁹	Mass movement deposit in the canyon axis.	
Ponta do Mel	2011	50	de Almedia et al. 2015 ⁵⁹		
Porto do Manguê	2011	50	de Almedia et al. 2015 ⁵⁹	Triangular landslide scars in the canyon head	

Macau	2011	50	de Almedia et al. 2015 ⁵⁹		<p>The figure is a topographic map of a canyon system. The upper portion is labeled 'Macau Canyon' and the lower portion 'Porto do Mangué Canyon'. A prominent 'border fault' is shown as a diagonal line separating the two canyon sections. The map features various gully types: 'feeding gullies' at the top, 'gullies' on a 'non excavated slope', 'well-developed gullies' in the middle, and 'wall gullies' on the right. A 'shelf edge' is marked with '1' at the top right. Elevation contours are marked with '1', '2', and '3' at different levels. A color scale on the right indicates elevation in meters, ranging from 200 (red) to 1,200 (blue). A scale bar at the bottom left shows 0, 2.5, and 5 km. A north arrow is in the top left corner. The letter 'A' is in the bottom left corner of the map area.</p>
-------	------	----	--------------------------------------	--	---

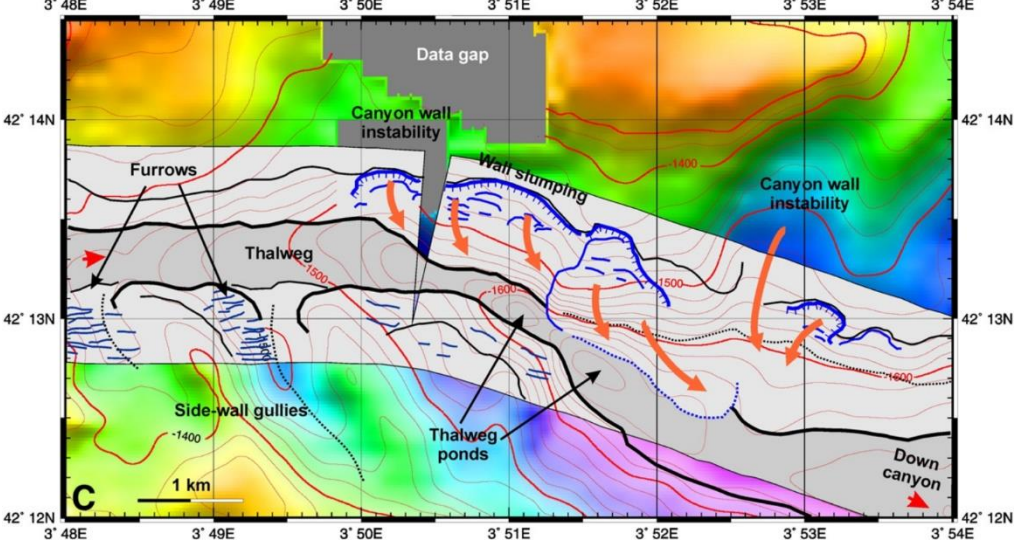
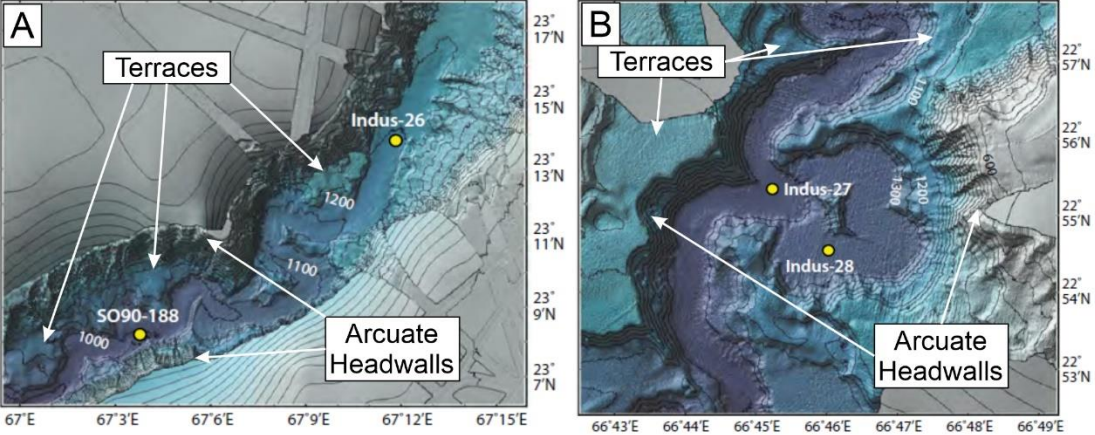
Acu	2011	50	de Almedia et al. 2015 ⁵⁹	Arcuate headwalls associated with terraces present.	
-----	------	----	--------------------------------------	---	--

Hattaras Transverse	2005, 2008, 2012	100	Gardner et al. 2016 ⁶⁰	Landslide scarps and deposits occur across large sections of the canyon. Deposits as high as 25 m down canyon of the confluence of the Hattaras Transverse and Lower Hattaras Canyons have impeded present flow down-canyon.	
Leven		10	Green and Uken, 2008 ⁶¹	Arcuate headwalls in canyon head and on mid-canyon walls.	

			Green, 2011 ⁶²	
Leadsman		10	Green and Uken, 2008 ⁶¹ Green, 2011 ⁶²	Arcuate headwalls in canyon head and on mid-canyon walls.
Diepgat		10	Green and Uken, 2008 ⁶¹ Green, 2011 ⁶²	Arcuate headwalls and terraces identifiable.
Wright		10	Green and Uken, 2008 ⁶¹ Green, 2011 ⁶²	Arcuate headwalls in canyon head and on mid-canyon walls.
White Sands		10	Green and Uken, 2008 ⁶¹	Landslide deposit visible in channel thalweg in

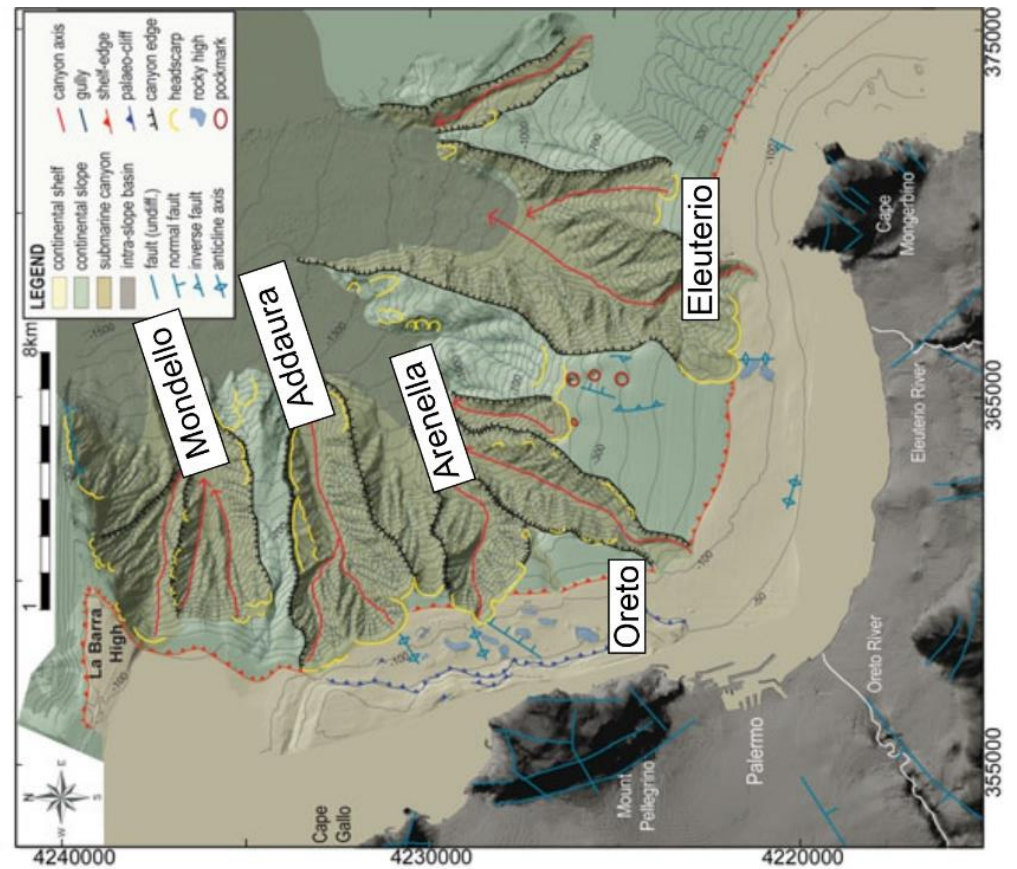


			Green, 2011 ⁶²	seismic reflection data.	
Mabibi		10	Green and Uken, 2008 ⁶¹ Green, 2011 ⁶²	Arcuate headwalls in canyon and on mid-canyon walls. Slump deposit in the canyon thalweg.	
Sur	1998	25	Harris et al. 2014 ⁶³	Arcuate landslide scars and multiple terraces visible.	
Partington	1998	25	Harris et al. 2014 ⁶³	Arcuate landslide scars and multiple terraces visible.	

Avon	2012		Jimoh et al. 2018 ⁶⁴	Sidewall scarps and terraces visible.	
Cap de Creus	1995, 2002, 2004	4, 50, 200	Lastras et al. 2007 ⁶⁵	Side wall slumping leading to narrowing of the canyon thalweg.	 <p>A topographic map of the Cap de Creus canyon. The map uses a color gradient from green (lower elevations) to red and orange (higher elevations). Key features are labeled: 'Furrows' (shallow depressions), 'Thalweg' (the main channel), 'Side-wall gullies' (small channels on the slopes), 'Thalweg ponds' (small pools in the channel), 'Wall slumping' (indicated by blue arrows and dashed lines), 'Canyon wall instability' (indicated by red arrows and dashed lines), and 'Down canyon' (indicated by a red arrow). A 'Data gap' is shown in a grey box at the top. A 1 km scale bar is located at the bottom left. The map is bounded by coordinates 3° 48'E to 3° 54'E and 42° 12'N to 42° 14'N.</p>
Indus	2008		Clift et al. 2014 ⁶⁶ Li et al. 2018 ⁶⁷	Terraces and arcuate scars visible. Slump deposits visible in seismic data.	 <p>Two panels, A and B, showing topographic maps of the Indus canyon. Panel A (left) shows a section of the canyon with labels for 'Terraces', 'Indus-26', 'SO90-188', and 'Arcuate Headwalls'. Panel B (right) shows another section with labels for 'Terraces', 'Indus-27', and 'Indus-28'. Both panels show contour lines and elevation markers (e.g., 1000, 1100, 1200, 1300). The maps are bounded by coordinates 66° 43'E to 67° 15'E and 22° 53'N to 23° 17'N.</p>

<p>Gaoping</p>			<p>Yeh et al. 2013⁶⁸</p> <p>Liu et al. 2016⁶⁹</p>	<p>Canyon-rim slumping and landslides visible in bathymetry. Slump deposits identified in seismic data.</p>	<p>The figure consists of two 3D bathymetric maps of Gaoping Canyon, oriented with North (N) at the top. The top map shows a wide view of the canyon with labels for 'turbidite deposit', 'boulder', 'minor channel', 'Kaoping Canyon', 'carbonate ridge', and 'channel cutting'. The bottom map provides a closer view of the canyon rim, highlighting 'landslide deposit', 'slumping cliff', and 'slope basin'. Both maps use a color scale to represent depth, with red and yellow indicating shallower areas and blue and purple indicating deeper areas.</p>
----------------	--	--	---	---	---

Mondello	2001, 2004, 2009	15	Lo lacono et al. 2011 ⁷⁰	Headscarps present at heads of gullies.
Addaura	2001, 2004, 2009	15	Lo lacono et al. 2011 ⁷⁰	Headscarps present along northern wall.

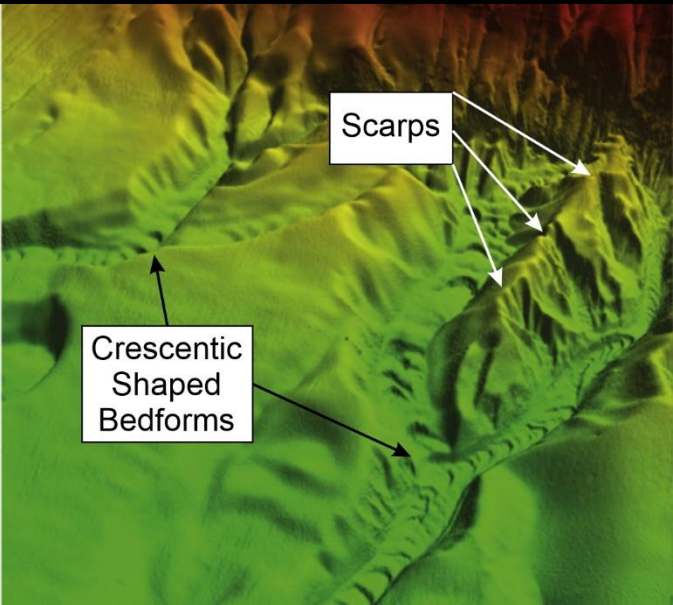


Oreto	2001, 2004, 2009	15	Lo Iacono et al. 2011 ⁷⁰	Headscarps visible. Obstruction clearly visible in canyon thalweg.	
Eleuterio	2001, 2004, 2009	15	Lo Iacono et al. 2011 ⁷⁰	Headscarps visible. 20 m high obstruction clearly visible in canyon thalweg.	
Cook	2002, 2005	10	Micallef et al. 2013 ⁷¹	Landslide scars clearly visible in bathymetry.	
Nicholson	2002, 2005	10	Micallef et al. 2013 ⁷¹	Landslide scars clearly visible in bathymetry.	
Wairarapa	2002, 2005	10	Micallef et al. 2013 ⁷¹	Landslide scars clearly visible in bathymetry.	

Campbell	2002, 2005	10	Micallef et al. 2013 ⁷¹	Landslide scars clearly visible in bathymetry.	
Palliser	2002, 2005	10	Micallef et al. 2013 ⁷¹	Landslide scars clearly visible in bathymetry. Landslide blocks are visible on canyon floor.	
Opouawe	2002, 2005	10	Micallef et al. 2013 ⁷¹	Landslide scars clearly visible in bathymetry.	
Embro Margin	1995, 1999	50	Micallef et al. 2014 ⁷²	Slide scars visible in bathymetry. Multiple terrace levels visible.	
Mona	1995, 2004	150	Mondziel et al. 2010 ⁷³	Landslide headscarps visible. Slump deposits	

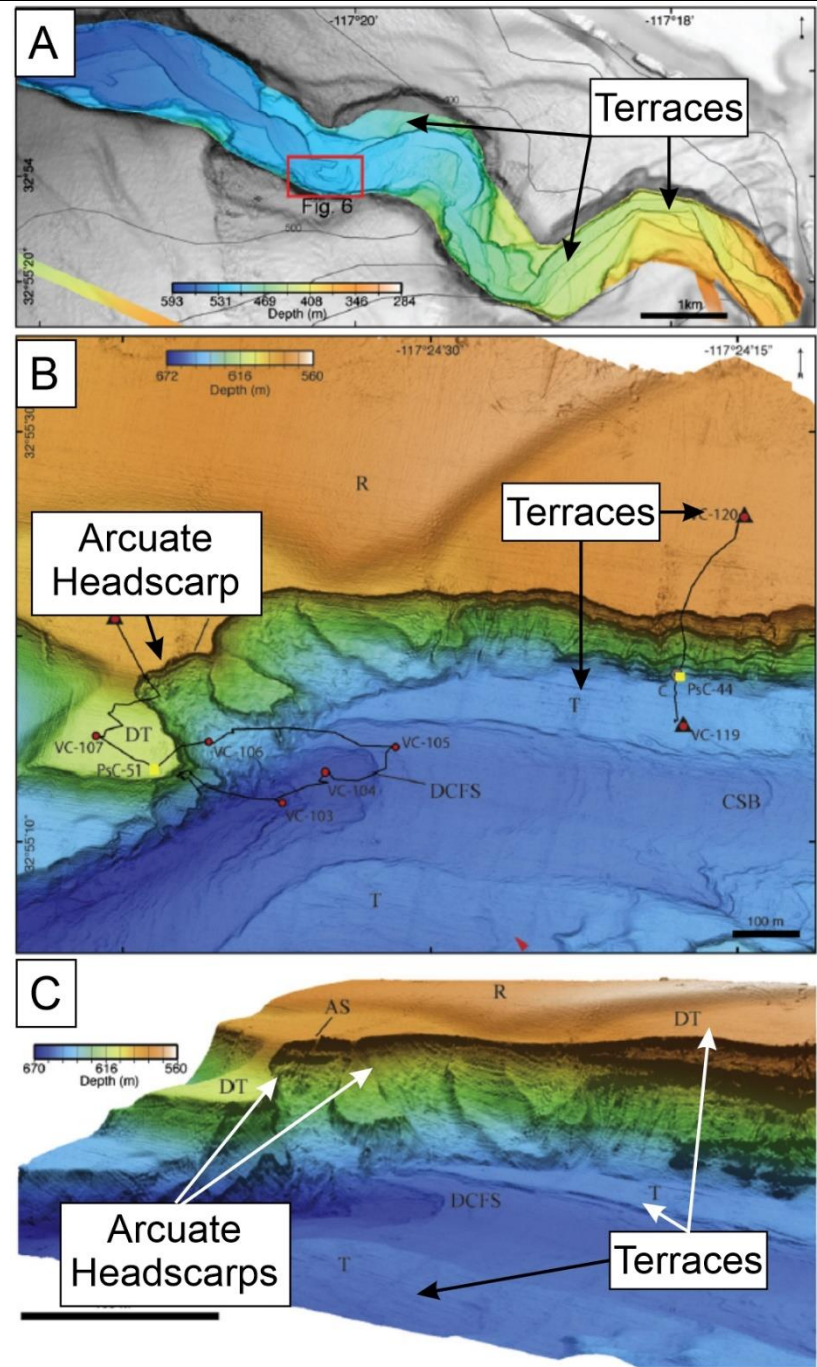
				visible in seismic data.	
Kaikoura	2018 (Repeat bathymetry)	25	Mountjoy et al. 2018 ¹¹	Canyon rim landslide evacuated through the canyon triggered by an earthquake.	<p>The figure consists of three panels labeled A, B, and C, illustrating bathymetric data of the Kaikoura Canyon. Panel A is a detailed map of the canyon area, showing sea floor change in meters. A color scale legend indicates erosion (red) and deposit (blue). The scale ranges from -40 m (dark red) to 20 m (dark blue), with 0 m in white. The map shows significant erosion (red) along the canyon rim and walls. Panel B is a zoomed-in view of the canyon rim, showing a 400 m scale bar. Panel C shows the Hundalee Fault, a prominent linear feature, with a 400 m scale bar. The location is marked as Kaikoura, and the longitude is given as 173°40' E.</p>

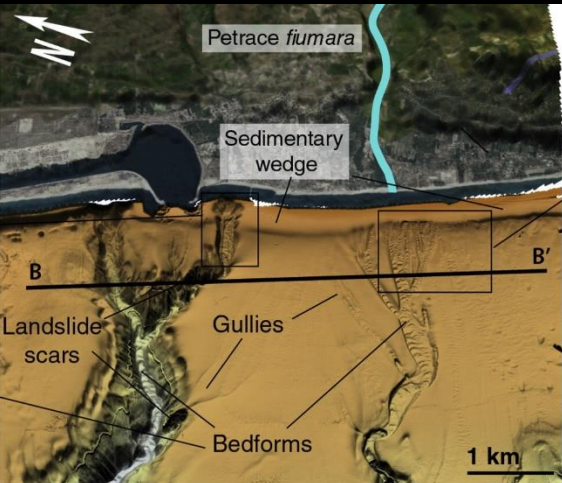
<p>Perth</p>	<p>2014, 2015, 2017, 2018</p> <p>(Repeat bathymetry in some areas)</p>	<p>20</p>	<p>Nanson et al. 2022⁷⁴</p>	<p>Landslide scars visible. Repeat bathymetry shows failures of some canyon headwalls due to earthquakes. Small accumulations of slump deposits visible in thalweg.</p>	<p>Change in seafloor pre- and post 2018</p> <p>Difference + 78 m - 61 m</p> <p>1 km</p> <p>Geomorphology map</p> <p>map limit, blind canyon, Escarpment, slump scar, fan levee, NP4, entrenched fan floor, cyclic step (or block), Slope, plunge pool (or block top), terrace dunes, slab, channel, gully network, Figure 13, sediment wave, Rottne Island, Swan River, Figure 12A, Figure 12B, Figure 14, map limit, 40 m grid (ship tracks), (inset: i), (inset: ii), 20 km, -5000 0</p> <table border="1"> <thead> <tr> <th>Morphology surfaces</th> <th>Geomorphology:</th> <th>Incisional</th> <th>Failure</th> <th>Aggradational</th> </tr> </thead> <tbody> <tr> <td>Plane</td> <td>channel</td> <td>palaeo-valley belt</td> <td>slab</td> <td>sediment wave</td> </tr> <tr> <td>Slope</td> <td>floor</td> <td>gully network</td> <td>slump scar</td> <td>cyclic step (or block)</td> </tr> <tr> <td>Escarpment</td> <td>plunge pool (or block top)</td> <td>entrenched floor</td> <td>block</td> <td>dunes</td> </tr> <tr> <td></td> <td>nick-point</td> <td>blind canyon</td> <td>creep</td> <td>levee</td> </tr> <tr> <td></td> <td></td> <td>terrace</td> <td></td> <td></td> </tr> </tbody> </table>	Morphology surfaces	Geomorphology:	Incisional	Failure	Aggradational	Plane	channel	palaeo-valley belt	slab	sediment wave	Slope	floor	gully network	slump scar	cyclic step (or block)	Escarpment	plunge pool (or block top)	entrenched floor	block	dunes		nick-point	blind canyon	creep	levee			terrace		
Morphology surfaces	Geomorphology:	Incisional	Failure	Aggradational																															
Plane	channel	palaeo-valley belt	slab	sediment wave																															
Slope	floor	gully network	slump scar	cyclic step (or block)																															
Escarpment	plunge pool (or block top)	entrenched floor	block	dunes																															
	nick-point	blind canyon	creep	levee																															
		terrace																																	

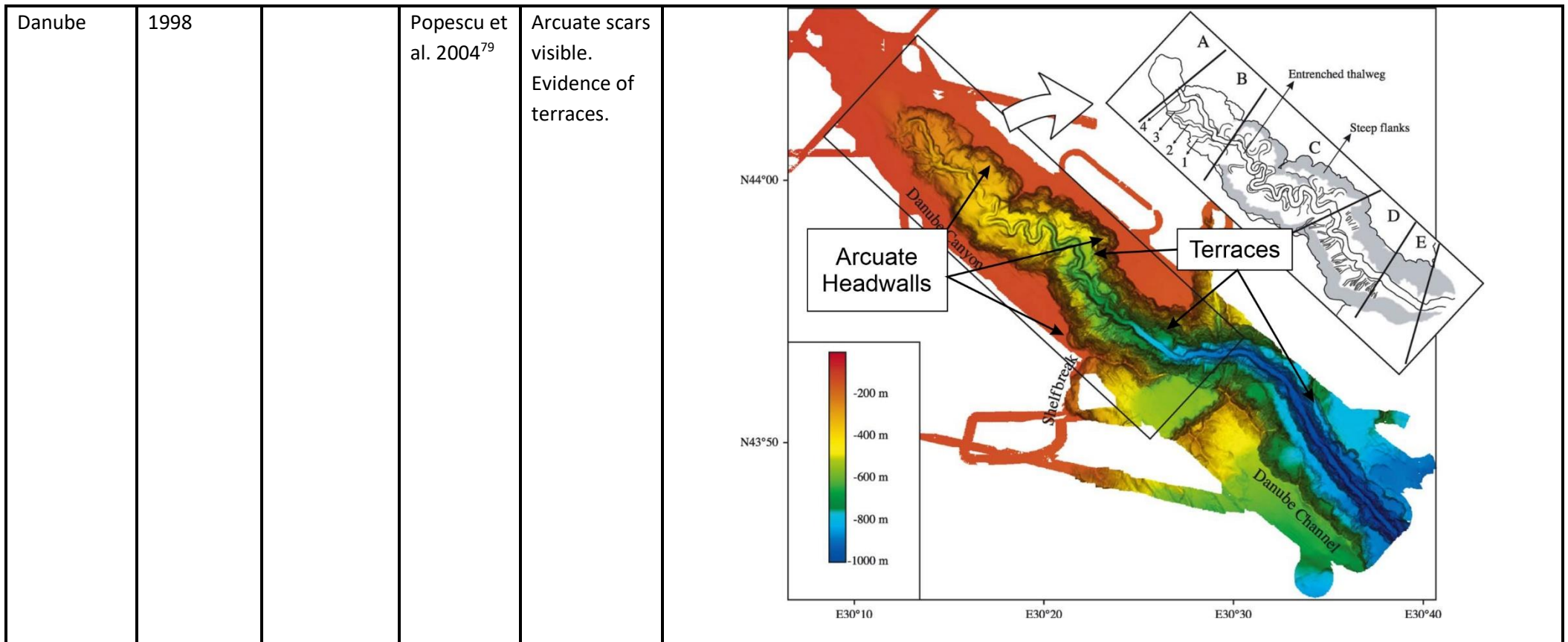
Pont-des-Monts	2007, 2012 (Repeat bathymetry)	3	Normandeau et al. 2014 ⁷⁵	Small scarps are visible.	
----------------	-----------------------------------	---	--------------------------------------	---------------------------	--

Goto	2008	25	Oiwane et al. 2011 ⁷⁶	Landslide headwalls observed in bathymetry.	
------	------	----	----------------------------------	---	--

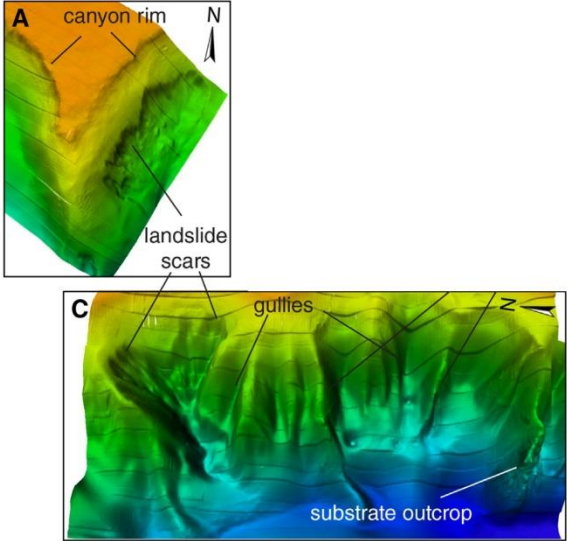
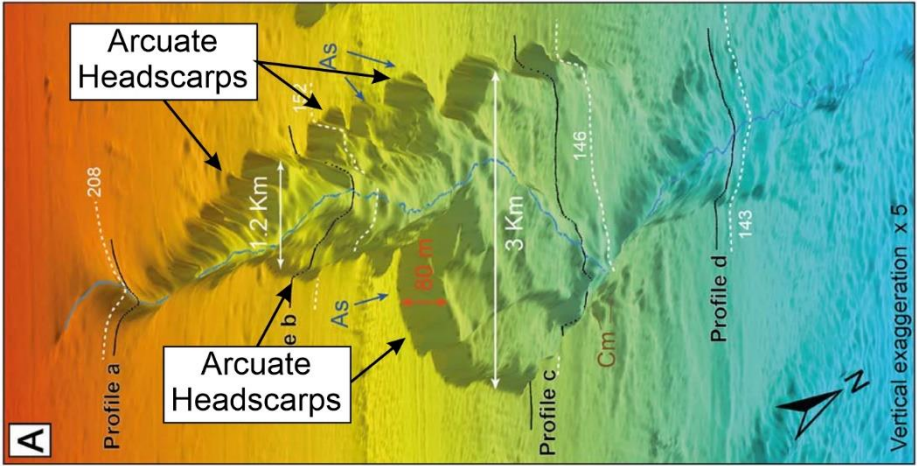
La Jolla	2008	0.7	Paull et al. 2013 ⁷⁷	Arcuate shaped scarps and terraces clearly visible.
----------	------	-----	---------------------------------	---

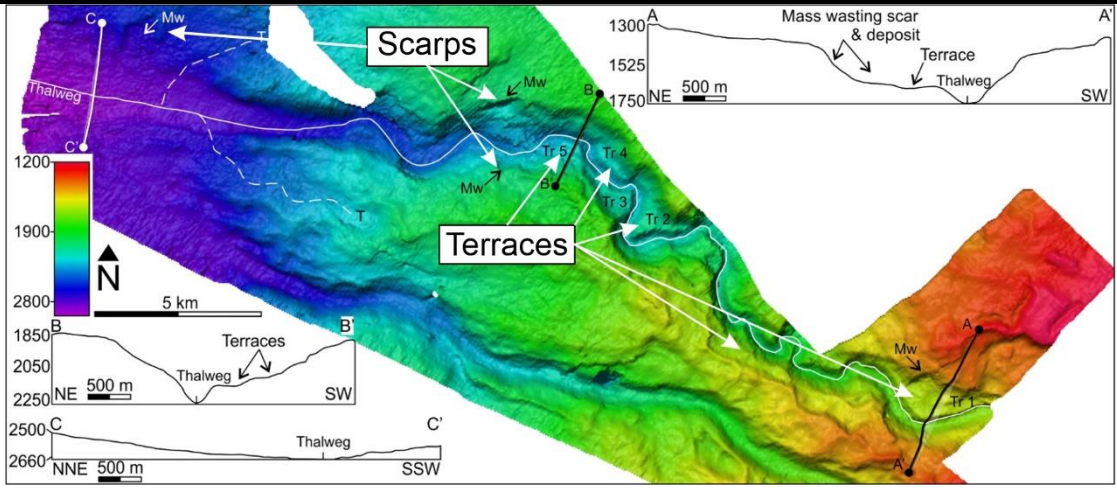
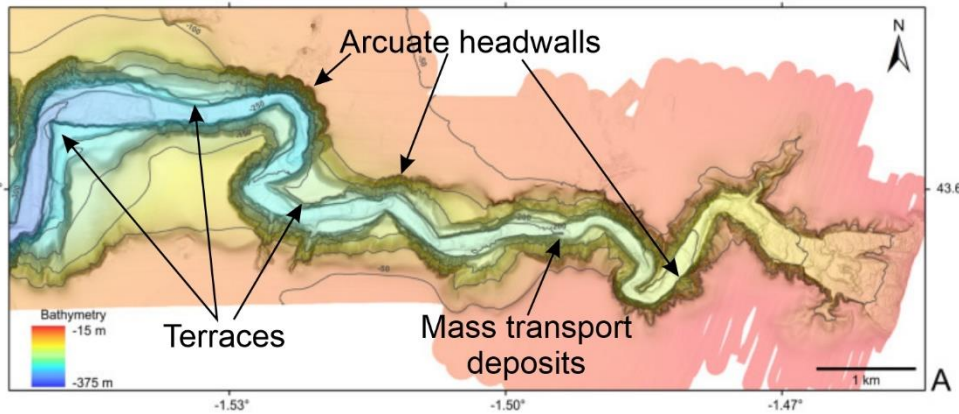


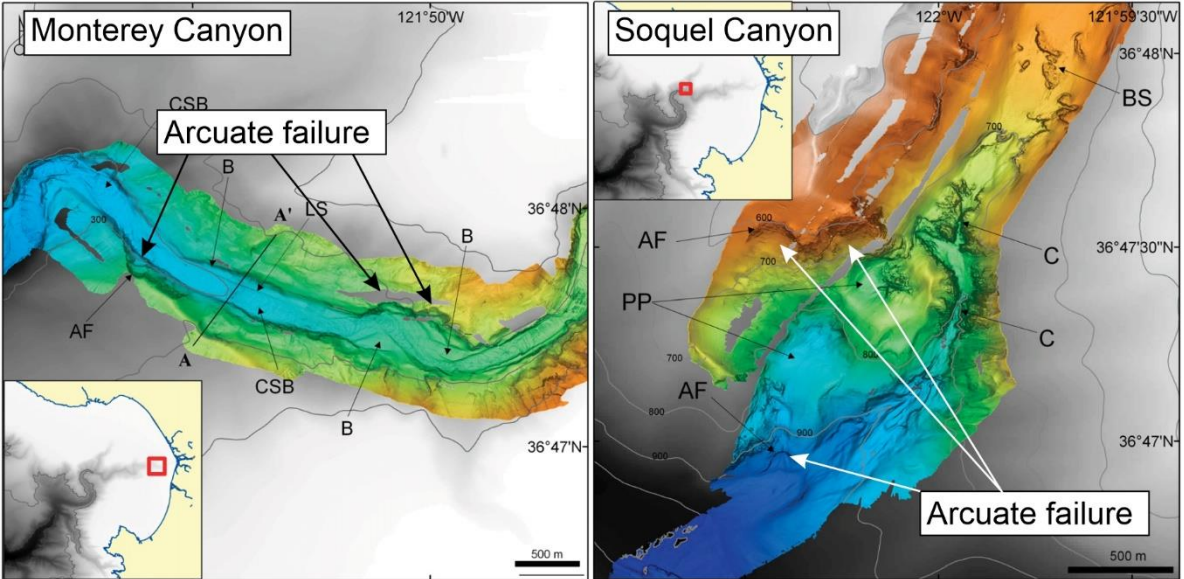
Gioia	2009, 2012	10	Pierdomenico et al. 2016 ⁷⁸	Landslide headwalls visible.	 <p data-bbox="1279 560 1839 598">Gioia Canyon Petrace Canyon</p>
-------	------------	----	--	------------------------------	---



Ribbon Reef	2007	40	Puga Bernabeu et al. 2011 ⁸⁰	Landslide headwalls visible in bathymetry. Suggested that knickpoints in canyon long profiles may be the result of slide deposits.	
Patia/Mira	2005	60	Ratzov et al. 2012 ⁸¹	Headscarps visible in bathymetry. Slump deposit has resulted in a canyon dam and infill visible in seismic data.	

Hudson	2007, 2008, 2009	3	Rona et al. 2015 ⁸²	Landslide scars visible on side walls.	 <p>Figure A: 3D topographic map showing a canyon rim (orange) and landslide scars (green/yellow) on the side walls. A north arrow is present.</p> <p>Figure C: 3D topographic map showing gullies (green/yellow) and a substrate outcrop (blue) at the base. A north arrow is present.</p>
São Vincente	2001 – 2009	250	Serra et al. 2020 ⁸³	Slide scars visible.	
Bahama Bank	2010	20	Tournadou r et al. 2017 ⁸⁴	Arcuate scarps visible.	 <p>Figure A: 3D topographic map of Bahama Bank showing arcuate headscarps. The map includes profiles a, b, c, and d. Distances of 1.2 Km and 3 Km are indicated. A vertical exaggeration of x 5 is noted. A north arrow is present.</p>

Mozambique Channel	2014	40	Wiles et al. 2019 ⁸⁵	Mass wasting scars identified on sidewalls.	 <p>This figure is a bathymetric map of a section of the Mozambique Channel. The map uses a color scale to represent depth, with shallower areas in red and orange, and deeper areas in blue and purple. Key features are labeled: 'Scarps' (steep slopes) and 'Terraces' (flatter, stepped areas). Specific terraces are labeled Tr 1 through Tr 5. Mass wasting scars (Mw) are also indicated. Three cross-sections are shown: A-A' at the top right, B-B' in the middle, and C-C' at the bottom. Each cross-section shows the profile of the channel floor and labels features like 'Mass wasting scar & deposit', 'Terrace', and 'Thalweg' (the deepest part of the channel). A 5 km scale bar and a north arrow are included.</p>
Capbreton	1998, 2020 (Repeat bathymetry)	0.5 - 5	Guiastrennec-Faugas et al. 2020 ⁶	Arcuate slide scars, slump scars and terraces	 <p>This figure is a bathymetric map of the Capbreton area. It shows a complex, winding channel system. Key features are labeled: 'Arcuate headwalls' (curved, steep slopes at the start of channel segments), 'Terraces' (flatter areas within the channel), and 'Mass transport deposits' (large, reddish-shaded areas on the right side of the map). A bathymetry scale is provided, ranging from -15 m (red) to -375 m (blue). The map includes a north arrow, a 1 km scale bar, and geographic coordinates: latitude 43.67° and longitude -1.53°, -1.50°, and -1.47°.</p>
Monterey	2008, 2009	1	Paull et al. 2011 ⁸⁶	Arcuate scars visible on canyon sidewalls	

Soquel	2008, 2009	1	Paull et al. 2011 ⁸⁶	Arcuate scars visible on canyon sidewalls	 <p>The figure consists of two bathymetric maps. The left map is titled 'Monterey Canyon' and shows a cross-section of the canyon with labels for 'CSB' (Canyon Side Bank), 'AF' (Arcuate Failure), 'A', 'A'', 'LS' (Lateral Scar), and 'B'. A box labeled 'Arcuate failure' has arrows pointing to several curved features on the canyon walls. The right map is titled 'Soquel Canyon' and shows a similar cross-section with labels for 'BS' (Basal Scar), 'AF', 'PP' (Pinnacled Point), and 'C'. A box labeled 'Arcuate failure' has arrows pointing to curved features on the canyon walls. Both maps include a 500 m scale bar and an inset map showing the canyon's location on a larger geographic scale.</p>
--------	------------	---	---------------------------------	---	--

38

39

40

41 STable. 2. Estimates of sediment and organic carbon masses displaced by submarine mass movement
 42 events, flood events and annual discharges from selected large rivers. The table demonstrates the
 43 efficiency of sediment and carbon capture and storage by the Congo Canyon landslide-dam.

		Displaced Mass (Mt)	Organic Carbon (Mt C)	Reference
Marine Settings				
Congo Canyon	Landslide	120±10	3.2 - 3.5 (min 3.1, max 3.8)	This study
Congo Canyon	Infill	170±40	4.6 - 5 (min 3.9, max 6.2)	This study
	Total	290±50	7.8 - 8.5 (min 7, max 10)	This study
Kaikōura Canyon/ Hikurangi Channel	2016 Kaikōura Earthquake/Landslide	850	7	Mountjoy et al. 2018
Continental shelf/ Japan Trench	2011 Tohoku-oki Earthquake/mass movement	360'	>1.73	Kioka et al. 2019
Fluvial Events				
Eel River	1995 flood	25	0.24	Leithold and Hope, 1999
North St. Vrain Creek	2013 flood	0.216	0.01	Rathburn et al. 2017
Kaoping River/Stored on floodplain	2009 Typhoon Morakot flood		0.72*	West et al. 2011
Kaoping River	2009 Typhoon Morakot flood		1.2 - 2.5*	West et al. 2011
Choshui River	2004 Typhoon Mindulle flood	61.4	0.5	Goldsmith et al. 2008
Annual fluvial discharge				
				Baudin et al. 2020 Coynel et al. 2005
Congo		43	2	Milliman and Farnsworth, 2011
				Bouchez et al. 2014
Amazon		900	11.5	Milliman and Farnsworth, 2011
				Wakeham et al. 2009 Rosenheim et al. 2013
Mississippi		210	9	Milliman and Farnsworth, 2011
				Li et al. 2015
Yangtze		478	4.4	Milliman and Farnsworth, 2011
				Galy et al. 2008 Galy and Eglinton, 2011
Ganges/Brahmaputra		1670	8	Milliman and Farnsworth, 2011
				Hilton et al. 2015
Mackenzie		100	2	Milliman and Farnsworth, 2011
				Galy et al. 2015
	Global Total	19,000 ± 500	200 +135/-75	Milliman and Farnsworth, 2011
Notes		*Coarse woody debris 'assumes density of 1,300 kg/m3		

44

45